Check for updates

Crystal structure, Hirshfeld surface analysis, and DFT studies of N-(2-chlorophenylcarbamothioyl)cyclohexanecarboxamide

Cemal Koray Ozer [iD] [1], Ummuhan Solmaz [iD] [2,*] and Hakan Arslan [iD] [1]

[1] Department of Chemistry, Faculty of Arts and Science, Mersin University, Mersin, TR 33343, Turkey
c.korayozer@gmail.com (C.K.O.), hakan.arslan@mersin.edu.tr (H.A.)
[2] Department of Chemistry and Chemical Processing Technologies, Technical Science Vocational School, Mersin University, Mersin, TR 33343, Turkey
ummuhansolmaz@mersin.edu.tr (U.S.)

* Corresponding author at: Department of Chemistry and Chemical Processing Technologies, Technical Science Vocational School, Mersin University, Mersin, TR 33343, Turkey.
 e-mail: ummuhansolmaz@mersin.edu.tr (U. Solmaz).

RESEARCH ARTICLE

ABSTRACT

N-(2-Chlorophenylcarbamothioyl)cyclohexanecarboxamide was characterized by a single crystal X-ray diffraction study. Crystal data for this compound, $C_{14}H_{17}ClN_2OS$; Monoclinic, space group $P2_1/n$ with $Z = 4$, $a = 5.2385(10)$ Å, $b = 17.902(4)$ Å, $c = 15.021(3)$ Å, $\beta = 90.86(3)°$, $V = 1408.5(5)$ Å³, $T = 153(2)$ K, μ(MoKα) = 0.413 mm⁻¹, $Dcalc = 1.400$ g/cm³, 9840 reflections measured ($7.082° \leq 2\theta \leq 50.378°$), 2519 unique ($R_{int} = 0.0406$, $R_{sigma} = 0.0335$) which were used in all calculations. The final R_1 was 0.0397 (I > 2σ(I)) and wR_2 was 0.0887 (all data). The puckering parameters ($q_2 = 0.019(3)$ Å, $q_3 = 0.578(3)$ Å, θ = 1.0(3)° and φ = 51(8)°) of the title compound show that the cyclohexane ring adopts a chair conformation. The molecular conformation of the title compound is stabilized by intramolecular hydrogen bonds (N2-H2⋯Cl1, N2-H2⋯O1, and C2-H2A⋯S1) and intermolecular hydrogen bonds (N1-H1⋯S1ⁱ and C9-HA⋯S1ⁱ i: 2-x, 2-y, 1-z). The intramolecular hydrogen bonds (N2-H2⋯O1 and C2-H2A⋯S1) are also form two pseudo-six-membered rings. Density functional theory optimized structure in the gaseous phase at B3LYP/6-311G(d,p) level of theory has been compared with the experimentally defined molecular structure. The molecular orbitals HOMO and LUMO with the energy gap for the title compound are calculated and the estimated energy gap (ΔE) between the HOMO and LUMO energies levels of the title compound is 3.5399 eV, which implies that the title molecule is very reactive. The Hirshfeld surface analysis reveals that the most important contributions to crystal packing are from H⋯H (49.0%), H⋯C/C⋯H (12.5%), H⋯Cl/Cl⋯H (10.9%), and H⋯S/S⋯H (10.0%) interactions. The energy-framework calculations are used to analyze and visualize the three-dimensional topology of the crystal packing. The intermolecular energy analysis confirmed a significant contribution of dispersion to the stabilization of molecular packings in the title compound.

1. Introduction

Coordination compounds have attracted a great deal of attention due to their structural variety, interesting physical and chemical properties, and promising applications in many fields [1,2]. Coordination compounds consist of a central atom and a ligand attached to the central atom. Among these, the N-benzoyl thiourea derivatives are versatile ligands that coordinate to form stable compounds. These derivatives possess very strong donor groups (Carbonyl and thioamide) that allow the preparation of different transition metal complexes, either monoanionic bidentate form by deprotonation that forms neutral homoleptic or heteroleptic complexes with S,O coordination or in neutral form only through the S atom [3-21]. Several benzoyl thiourea derivatives and their metal complexes are also associated with various types of biological activities such as insecticidal, herbicidal, antibacterial, antifungal, anti-

tubercular, antithyroid, anthelmintic, rodenticidal, and plant growth regulator properties [22-25].

Our colleagues have pursued investigations on the synthesis, characterization, thermal behavior, antimicrobial activity, and catalytic activity of benzoyl thiourea derivatives [26-35]. Based upon the literature search, we could find no crystal structure characterization of N-(2-chlorophenyl-carbamothioyl)cyclohexanecarboxamide compound except reference [28]. In this work, in continuation of our ongoing interest in structural studies of thiourea derivative molecules [26-35], we re-refined and report the single-crystal X-ray diffraction study of the title compound. In addition, density functional theory optimized structure in the gaseous phase at B3LYP/6-311G(d,p) level has been compared with the experimentally defined new re-refined molecular structure. A Hirshfeld surface analysis and energy framework study was also performed to complement the experimental results to attempt to understand the nature of the described noncovalent
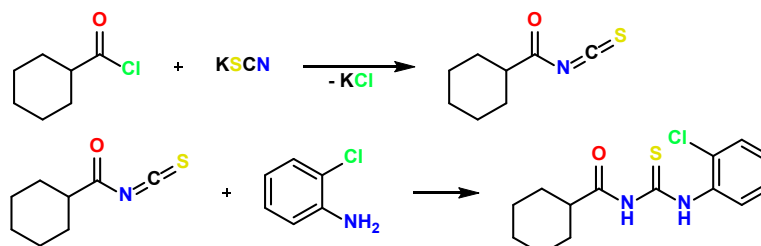
Scheme 1. Synthesis of the title compound (H₂L).
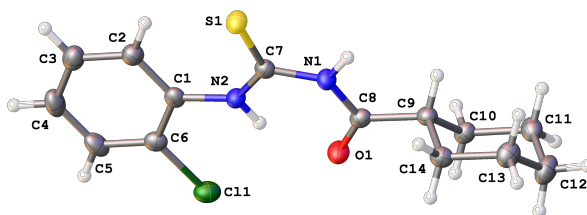
Figure 1. The molecular structure of the title compound.

interactions in the supramolecular network of the title compound.

2. Experimental

2.1. Instrumentation

The X-ray single-crystal diffraction data were recorded on a Rigaku Mercury AFC8S system with a Mercury CCD detector. A suitable crystal was selected and mounted onto a Nylon loop on a Rigaku Mercury system. The crystal was kept at T = 153(2) K during data collection. Data were collected with graphite-monochromated MoKα radiation ($λ$ = 0.71073 Å). Using Olex2 [36], the structure was solved with the Superflip [37-39] structure solution program, using the Charge Flipping solution method, and refined by the full-matrix least squares technique on F^2 using SHELXL [40] with refinement of F^2 against all reflections. All non-H atoms were refined anisotropically. ORTEP views were drawn using OLEX2 software [36].

2.2. Synthesis

The compound was reported in a previous study in the literature [27]. A solution of cyclohexanecarbonyl chloride (0.005 mole) in acetone (50 mL) was added dropwise to a suspension of potassium thiocyanate (0.005 mole) in acetone (50 mL). The reaction mixture was heated under reflux for 30 min and then cooled to room temperature. A solution of 2-chloro benzylamine (0.005 mole) in acetone (30 mL) was added to the mixture for 15 min at room temperature and stirred for 2 h. Hydrochloric acid (0.1 N, 300 mL) was added and the solution was filtered. The solid product was washed with water and purified by recrystallization from an ethanol:dichloro methane mixture (1:2, v:v) (Scheme 1). Color: White. Yield: 93 %. M.p.: 136-138 °C.

2.3. Computational studies

The density functional theory calculations for the title compound were performed using Gaussian 16 software [41]. They were carried out with Becke three parameters for the exchange with correlation functional of Lee-Yang-Parr (B3LYP) for 6-311G(d,p) basis set [42,43]. The Gauss View 06 program [44] was used to visualize the calculated parameters. All the parameters were allowed to relax, and all the calculations converged to an optimized geometry. The local minima were confirmed by the absence of an imaginary mode in the vibrational analysis calculations. Hirshfeld surfaces [45,46] was performed with the aid of CrystalExplorer 17.5 software [47] to verify the contributions of different intermolecular interactions. The two-dimensional fingerprint plots [48] were calculated using the crystallographic information file as input for analysis. Electrostatic potentials were calculated using Gaussian 16 and TONTO [41,49,50] and mapped on Hirshfeld surfaces using the 6-311G(d,p) basis set at the B3LYP level of theory. On the surfaces, donors with positive potential (blue regions) and acceptors with negative potential (red regions) are represented. The proposed molecular structure's with Hirshfeld surfaces (Shape index and curvedness), map over the shape index region −1.000 to 1.000 Å and the curvedness region −4.000 to +0.400 Å. For the generation of fingerprint plots, the bond lengths of hydrogen atoms involved in the interactions were normalized to standard neutron values [51]. The 2D fingerprint plots were displayed using the standard view with the d_e and d_i distance scales displayed on the graph axes. The energies of intermolecular interaction of the molecular pairs in the crystal packing were calculated using 3D energy framework analysis, at B3LYP/6-311G(d,p) level of theory, in a cluster of radius 3.8 Å around the molecule. The neighboring molecules in the shell around the central molecule were generated by applying crystallography symmetry operations.

3. Result and discussion

3.1. Crystal structure analysis

The title compound was prepared and characterized previously [27]. To the best of our knowledge, no reports on the single crystal of this molecule exist except reference [28]. As a follow-up to the synthesis and characterization, a recrystallization of an authenticated this molecule with dichloromethane and ethanol was undertaken. A suitable single crystal of the title compound for the X-ray diffraction study was obtained by slow evaporation of a dichloromethane:ethanole (1:2, *v:v*) solution [27,28]. The re-refined molecular structure of the compound in crystal form with the corresponding atom numbering scheme is shown in Figure 1 and the crystal packing of the compound is viewed along the crystal *a*-axis and *c*-axis in Figure 2.

Table 1. Crystallographic data and refinement parameters for the title compound.

Parameters	H_2L
Empirical formula	$C_{14}H_{17}ClN_2OS$
Formula weight	296.81
Temperature (K)	153(2)
Crystal system	Monoclinic
Space group	$P2_1/n$
a, (Å)	5.2385(10)
b, (Å)	17.902(4)
c, (Å)	15.021(3)
β, (°)	90.86(3)
Volume (Å³)	1408.5(5)
Z	4
ρ_{calc} (g/cm³)	1.400
μ (mm⁻¹)	0.413
F (000)	624.0
Crystal size (mm³)	0.72 × 0.19 × 0.12
Radiation	MoKα (λ = 0.71073)
2Θ range for data collection (°)	7.082 to 50.378
Index ranges	$-6 \leq h \leq 6, -21 \leq k \leq 20, -15 \leq l \leq 17$
Reflections collected	9840
Independent reflections	2519 [R_{int} = 0.0406, R_{sigma} = 0.0335]
Data/restraints/parameters	2519/0/240
Goodness-of-fit on F²	1.137
Final R indexes [I≥2σ (I)]	R_1 = 0.0397, wR_2 = 0.0844
Final R indexes [all data]	R_1 = 0.0503, wR_2 = 0.0887
Largest diff. peak/hole (e Å⁻³)	0.26/-0.27

Table 2. The experimental and theoretical bond lengths of the title compound.

Atom	Atom	Length (Å)		Atom	Atom	Length (Å)	
		Experimental (X-ray)	Theoretical (DFT)			Experimental (X-ray)	Theoretical (DFT)
O1	C8	1.227(3)	1.2230	C3	C4	1.384(4)	1.3916
Cl1	C6	1.739(2)	1.7596	C4	C5	1.383(4)	1.3908
S1	C7	1.669(2)	1.6729	C5	C6	1.381(3)	1.3887
N1	C7	1.389(3)	1.4082	C8	C9	1.512(3)	1.5205
N1	C8	1.376(3)	1.3827	C9	C10	1.525(3)	1.5457
N2	C1	1.410(3)	1.4094	C9	C14	1.539(3)	1.5442
N2	C7	1.346(3)	1.3501	C10	C11	1.526(3)	1.5345
C1	C2	1.398(3)	1.4002	C11	C12	1.519(4)	1.5344
C1	C6	1.409(3)	1.4066	C12	C13	1.522(4)	1.5345
C2	C3	1.392(3)	1.3896	C13	C14	1.525(3)	1.5347

Table 3. The experimental and theoretical bond angles of the title compound.

Atom	Atom	Atom	Angle (°)		Atom	Atom	Atom	Angle (°)	
			Experimental (X-ray)	Theoretical (DFT)				Experimental (X-ray)	Theoretical (DFT)
C8	N1	C7	129.53(19)	130.1560	N2	C7	S1	128.15(17)	129.1519
C7	N2	C1	131.0(2)	129.7756	N2	C7	N1	114.21(19)	113.8546
C2	C1	N2	124.84(19)	123.5793	O1	C8	N1	122.65(19)	122.7877
C2	C1	C6	118.0(2)	117.8269	O1	C8	C9	123.03(19)	121.9433
C6	C1	N2	117.15(19)	118.5297	N1	C8	C9	114.31(18)	115.2666
C3	C2	C1	120.2(2)	120.7162	C8	C9	C10	112.12(18)	109.4879
C4	C3	C2	121.0(2)	120.6465	C8	C9	C14	109.75(17)	110.0766
C5	C4	C3	119.3(2)	119.5372	C10	C9	C14	110.99(18)	110.8440
C6	C5	C4	120.4(2)	119.8060	C9	C10	C11	110.06(18)	111.5439
C1	C6	Cl1	120.24(17)	120.1909	C12	C11	C10	110.8(2)	111.6577
C5	C6	Cl1	118.70(18)	118.3458	C11	C12	C13	111.8(2)	111.2614
C5	C6	C1	121.0(2)	121.4632	C12	C13	C14	110.9(2)	111.7023
N1	C7	S1	117.64(15)	116.9900	C13	C14	C9	110.75(19)	111.5024

Crystallographic data and new refinement parameters are summarized in Table 1, and the bond length and angle parameters are tabulated in Tables 2 and 3.

In the molecular structure of the title compound, the bond lengths of carbonyl (C8-O1) and thiocarbonyl are 1.227(3) and 1.669(2) Å, which are found in the range of typical double bonds for the C=O and C=S groups, respectively [26-28,52,53]. The C-N bond lengths for this molecule (C8-N1: 1.376(3) Å, C7-N1: 1.389(3) Å, C7-N2: 1.346(3) Å, C1-N2: 1.410(3) Å) are all shorter than the average single C–N bond length of 1.48 Å, thus showing varying degrees of double bond character in these C-N bonds [54-58]. The bond lengths within the cyclohexane ring (C9-C14) lie in the expected lengths (C9-C10: 1.525(3), C10-C11: 1.526(3), C11-C12: 1.519(4), C12-C13: 1.522(4), C13-C14: 1.525(3), C9-C14: 1.539(3) Å). The bond angles in cyclohexane ring (C9-C14) are in the range between 110.06(18) and 111.8(2)° and these obtained bond angle values agree with the literature values [26-28]. The puckering parameters are q_2 = 0.019(3) Å, q_3 = 0.578(3) Å, θ = 1.0(3)°, and φ = 51(8)°. The

conformation of the cyclohexane ring slightly deviates from the ideal chair (θ = 1.0(3)°) for the title compound. These ring puckering parameters show that the cyclohexane ring has a chair conformation [59,60].

The crystal packing of the title compound is stabilized by a combination of intramolecular and intermolecular hydrogen bonds (Table 4). The intramolecular hydrogen bonds cause the formation of the two fused $S(6)$ ring motifs in the title compound (Figure 3).

3.2. Computational studies

The bond angles and bond lengths of the experimental XRD and DFT optimized title compound are listed in Tables 2 and 3. The theoretical and experimental parameters differ somewhat, which may be explained by the fact that the DFT calculation was performed on an isolated molecule in the gaseous phase, whereas the X-ray parameters were calculated on molecules in the solid-state (Figure 4).

Table 4. Intra- and inter-molecular hydrogen bonds for the title compound (Å, °).

D-H···A	d(D-H)	d(H···A)	d(D···A)	∠ D-H···A	Symmetry
N(1)-H(1)···S(1)	0.77(3)	2.71(3)	3.4679(19)	166(2)	2-*x*, 2-*y*, 1-*z*
N(2)-H(2)···Cl(1)	0.84(3)	2.44(3)	2.9389(19)	116(2)	-
N(2)-H(2)···O(1)	0.84(3)	1.91(3)	2.646(2)	145(2)	-
C(2)-H(2A)···S(1)	0.92(3)	2.58(3)	3.192(2)	125(2)	-
C(9)-H(9)···S(1)	0.99(2)	2.82(2)	3.561(2)	132.2(16)	2-*x*, 2-*y*, 1-*z*

(a)   (b)
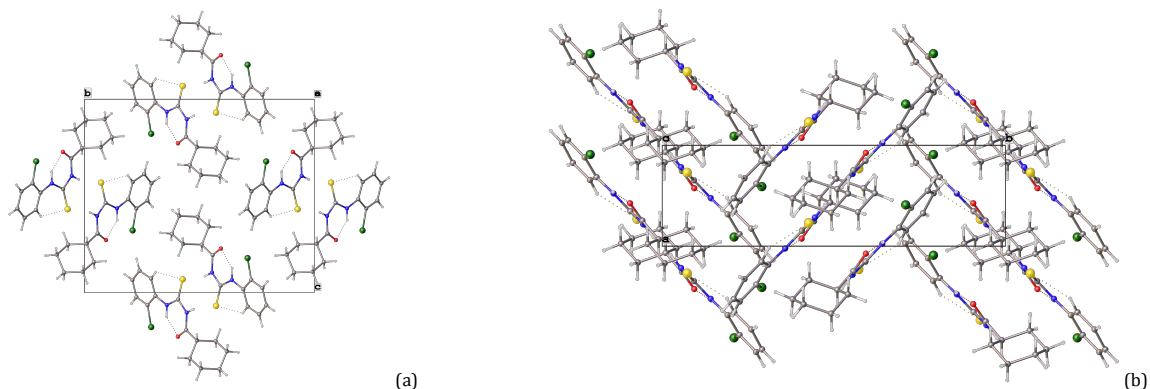
Figure 2. The unit cell packing of the title compound viewed along the *a*-axis (a) and *c*-axis (b).
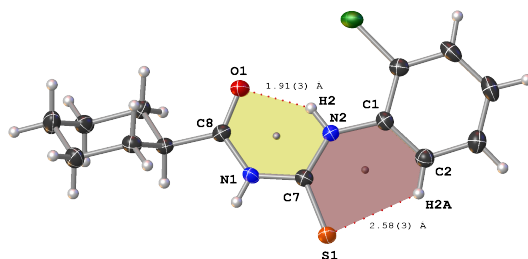
Figure 3. Intramolecular hydrogen bonds cause the formation of two fused *S*(6) ring motifs in the title compound.
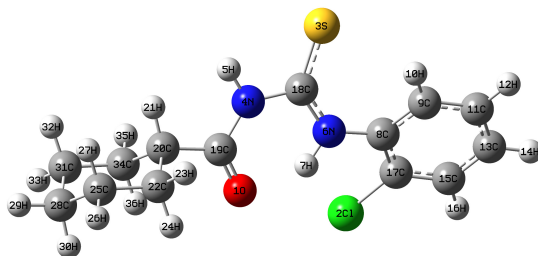
Figure 4. Optimized geometric structure of the title compound obtained at B3LYP/6-311G(d,p) level.
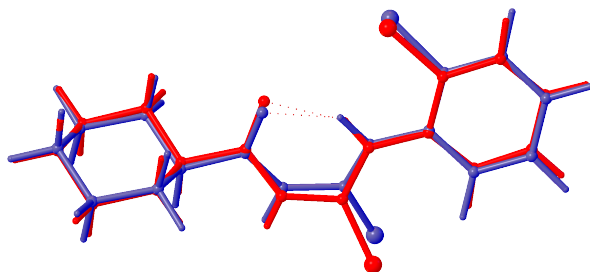
Figure 5. Atom-by-atom superimposition of the structures calculated (blue) over the X-ray structure (red) for the title compound.

The experimental geometries determined by the X-ray diffraction technique and the theoretically derived geometries overlapped in the current study (Figure 5). In the bond length calculations, the correlation was found at the B3LYP/6-311G(d,p) level of theory as r = 0.9987, and the maximum difference between the theoretical and experimental bond lengths (C9-C10) was 0.0207 Å. In the bond angle calculations, the correlation was found as r = 0.9888, and the maximum

difference between the theoretical and experimental bond angles (C8-C9-C10) was 2.632°. The RMS value resulting from the superposition of the experimental and theoretically structure was found to be 0.452 Å for B3LYP/6-311G(d,p) level. According to this result, the DFT method has minor level error and we can use for the future calculations for the characterization of the three-dimensional structure of molecular geometry.

Table 5. Calculated energy values and quantum molecular descriptors of the title compound.

Parameters	Values
SCF energy (a.u.)	-1587.13
Total energy (Thermal) E_{total} (kcal/mol)	195.16
Heat capacity at const. volume, C_v (cal/mol.K)	67.377
Vibrational energy, E_{vib} (kcal/mol)	193.383
Zero-point vibrational energy, E^o (kcal/mol)	184.102
Entropy (cal/mol.K)	
Translational	42.954
Rotational	34.633
Vibrational	63.660
Total	141.247
Rotational constant (GHz)	
A	0.62251
B	0.14267
C	0.12408
Dipole moment (Debye)	
μ_x	-2.2665
μ_y	-0.5163
μ_z	1.0532
μ_{Total}	2.5520
LUMO energy (eV)	-2.1701
HOMO energy (eV)	-5.7100
Energy gap (eV)	3.5399
Ionization potential (eV)	5.7100
Electron affinity (eV)	2.1701
Chemical hardness (eV)	1.7700
Global softness (1/eV)	0.2825
Electronegativity (eV)	3.9401
Chemical potential (eV)	-3.9401
Electrophilicity (eV)	4.3854

E_{LUMO} = -2.1701 eV

↕ ΔE = 3.5399 eV

E_{HOMO} = -5.7100 eV
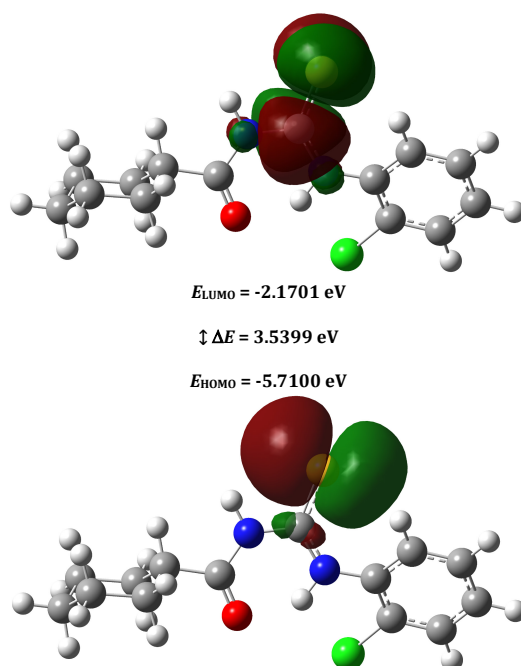
Figure 6. HOMO-LUMO energy levels and energy gap of the title compound.

In addition, the global chemical reactivity descriptors enable us to know the chemical properties of the title compound. Therefore, DFT/B3LYP/6-311G(d,p) platform was used to obtain the quantum mechanical molecular energy data and the data obtained are incorporated in Table 5.

The frontier molecular orbitals highest occupied molecular orbital (HOMO) and lowest unoccupied molecular orbital (LUMO) of the title compound were generated. The energy gap between the molecular orbitals describes the chemical reactivity and chemical stability of the related molecule. It is clear that a molecule with a low-energy gap is expected to be more polarizable and associated with a high chemical reactivity [61]. The molecular orbitals HOMO and LUMO with the energy gap for the title compound are shown in Figure 6. The estimated energy gap (ΔE) between the HOMO and LUMO energies levels

of the title compound is 3.5399 eV, which implies that the molecule is more chemically reactive and unstable. In addition, this lower energy gap explains the easy transfer of electrons taking place within the title molecule.

Hirshfeld surface analysis has been conducted to verify the contributions of different intermolecular interactions in forming supramolecular structure. The intermolecular interactions in the re-refined crystal structure of the title compound have been examined using Hirshfeld surface analysis and fingerprint plots utilizing Crystal Explorer 17.5 [47]. Fingerprint plots with d_{norm} surfaces (where $d_{norm} = d_i + d_e$) for all intermolecular contacts, and the intermolecular energies of the molecular pairs in the crystal packing were calculated with molecular wavefunction at the B3LYP/6-311G(d,p) level of theory, cluster of radius 3.8 Å around the molecule.
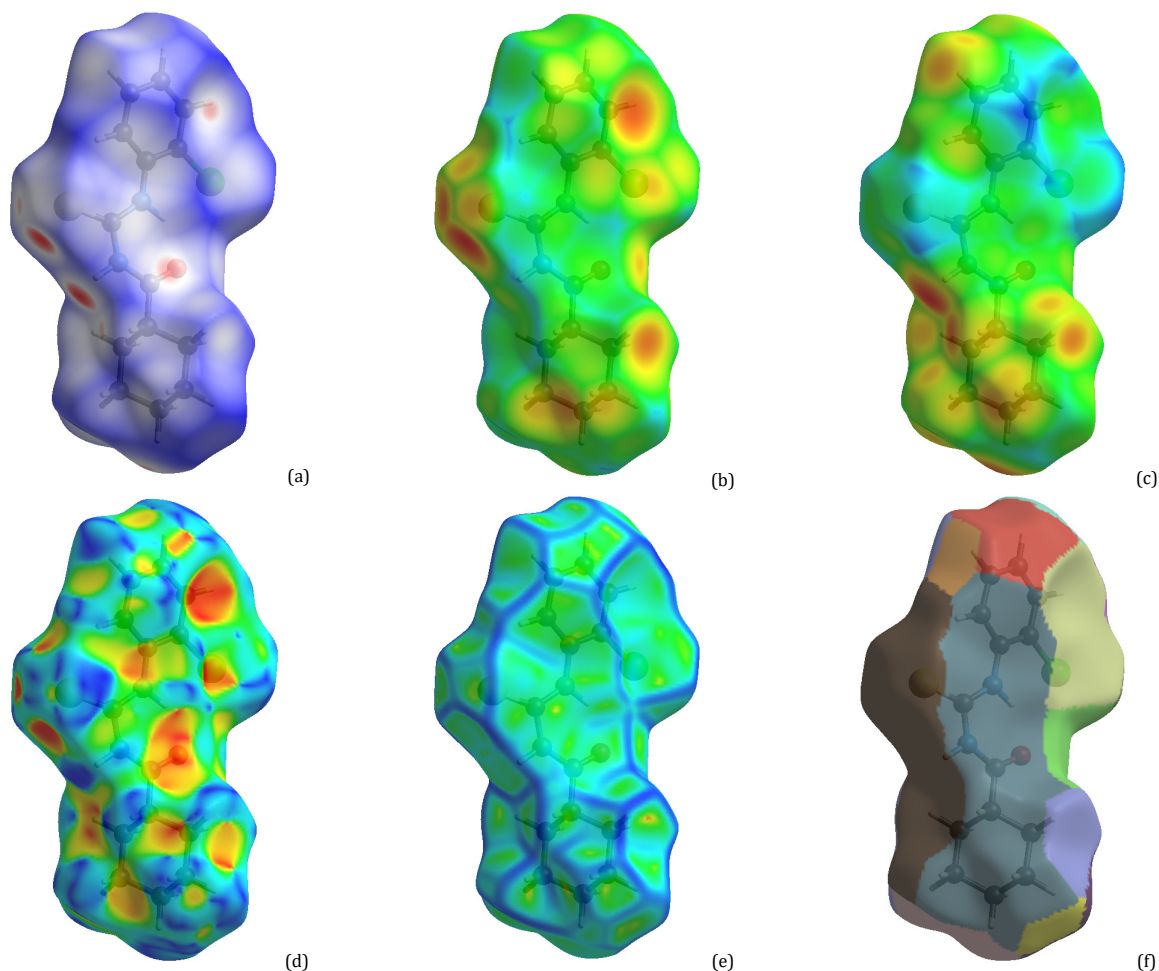
Figure 7. Hirshfeld surfaces mapped with d_{norm} (a), d_e (b), d_i (c), shape index (d), curvedness (e) and fragment patch (f) for the title compound.
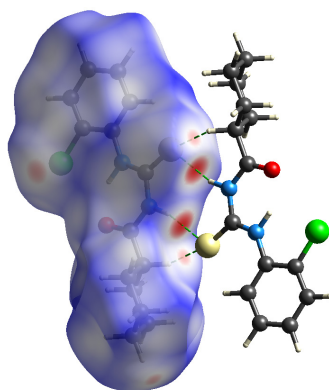
Figure 8. d_{norm} map showing regions intermolecular contacts over the title compound.

The Hirshfeld surfaces of the title compound have been mapped over d_{norm}, d_e, d_i, shape index, and curvedness (Figure 7). The d_{norm} value is positive for longer contacts (blue region, d_{norm} > VdW radii), negative for shorter contacts (red regions, d_{norm} < VdW radii) compared to van der Waals separation (white regions, d_{norm} = VdW radii). The calculated molecular Hirshfeld surface area is 322.08 Å², which encloses the volume of 345.22 Å³. Other calculated shape descriptors are globularity G = 0.739 and asphericity Ω = 0.316. The term asphericity is a measure of structural anisotropy, and globularity is found as < 1, indicating that the molecular surface is more structured [62-64]. Figure 8 displays semitransparent d_{norm}-mapped the Hirshfeld surface

for the title compound that form strong intermolecular contacts. The red regions in Figure 8 are apparent around the sulphur atom participating in the C-H···S and N-H···S contacts.

The 2D fingerprint plot provides a precise two-dimensional graphical representation of the intermolecular interactions in the crystal. The contributions from different contacts to the total Hirshfeld surface area are H···H (49.0%), H···C/C···H (12.5%), H···Cl/Cl···H (10.9%), H···S/S···H (10.0%), H···O/O···H (7.0%), and H···N/N···H (1.6%). The general contributions of the different contacts to the total Hirshfeld surface area are shown in Figure 9.
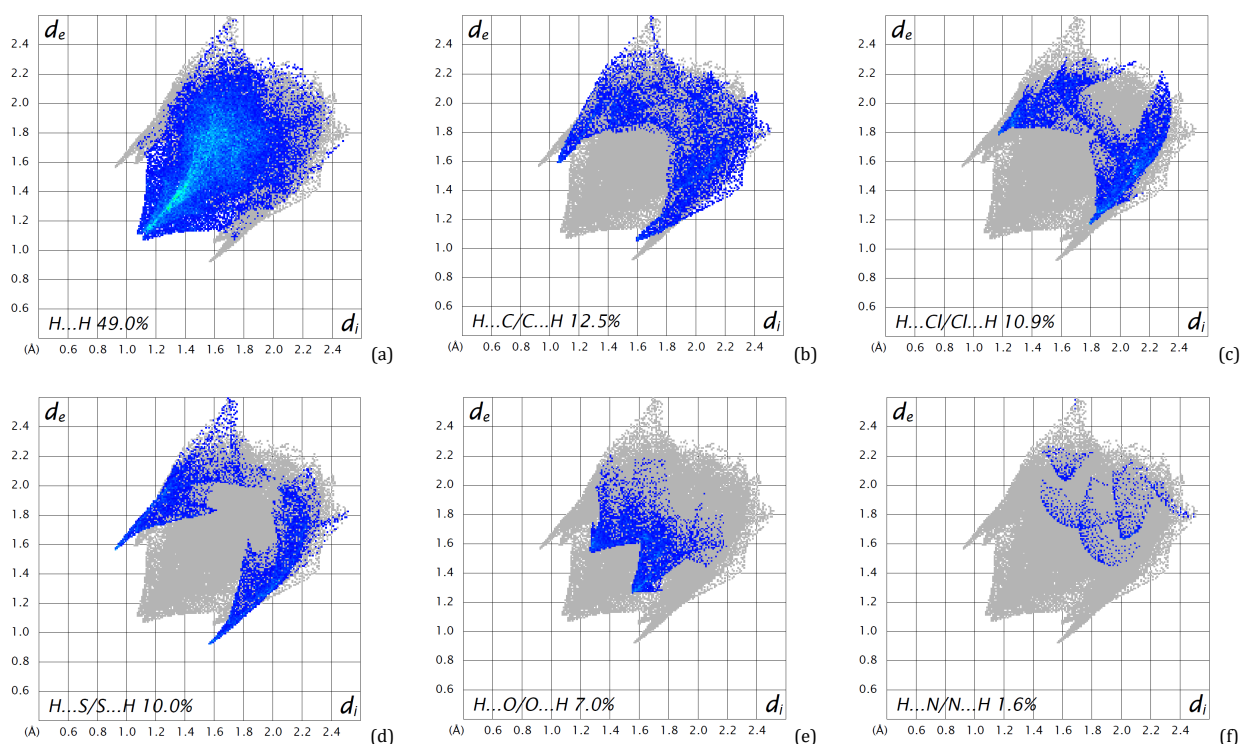
Figure 9. 2-Dimensional fingerprint plot of the main intermolecular interactions in the crystal structure of the title compound.
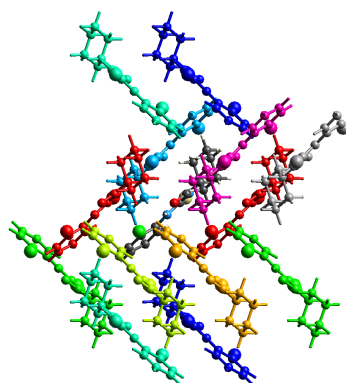
Figure 10. Molecular pairs involved in the calculation of interaction energies of the title compound along the *c* axis.

Table 6. Different interaction energies of molecular pairs in kJ/mol.

Color *	Symmetry	Electron density	R	E_{ele}	E_{pol}	E_{dis}	E_{rep}	E_{tot}
	x, y, z	B3LYP/6-311G(d,p)	5.24	-17.60	-3.90	-60.10	55.20	-26.40
	x+1/2, -*y*+1/2, *z*+1/2	B3LYP/6-311G(d,p)	9.47	-4.20	-1.00	-12.40	5.30	-12.30
	x+1/2, -*y*+1/2, *z*+1/2	B3LYP/6-311G(d,p)	9.53	-1.50	-0.20	-5.60	4.10	-3.20
	x+1/2, -*y*+1/2, *z*+1/2	B3LYP/6-311G(d,p)	11.97	0.20	-0.30	-6.70	4.20	-2.60
	-*x*+1/2, *y*+1/2, -*z*+1/2	B3LYP/6-311G(d,p)	10.22	-2.10	-0.50	-11.50	7.90	-6.20
	-*x*, -*y*, -*z*	B3LYP/6-311G(d,p)	5.41	-31.30	-5.70	-45.70	58.70	-24.00
	x+1/2, -*y*+1/2, *z*+1/2	B3LYP/6-311G(d,p)	9.87	-7.60	-0.50	-18.50	18.40	-8.20
	-*x*, -*y*, -*z*	B3LYP/6-311G(d,p)	7.12	-78.10	-10.40	-33.30	106.80	-15.00
	-*x*, -*y*, -*z*	B3LYP/6-311G(d,p)	12.60	-4.50	-0.50	-19.90	17.20	-7.70

* The color and compound relationship is given in Figure 10.

Molecular pairs involved in the calculation of the interaction energies of the title compound along the *c* axis are shown in Figure 10 (Table 6). The pictorial representation of Coulomb energy, dispersion energy, and the total interaction energy of the molecule viewed along *a*, *b*, and *c* axis is shown in green, red, and blue colors, respectively, and are displayed in Figure 11. The total intermolecular interaction energy (E_{tot}) is the sum of four energy terms: electrostatic (E_{ele}), polarization (E_{pol}), dispersion (E_{disp}) and exchange-repulsion (E_{rep}) with scale factors of 1.057, 0.740, 0.871, and 0.618, respectively [65].

The different interaction energies *viz.*, electrostatic, polarization, dispersion, and repulsion energies are -146.7, -23.0, -213.7, and 277.8 kJ/mol, respectively. The total energy is -105.6 kJ/mol. The cylinders in the energy framework depict the relative strengths of the molecular packing and the associated energies between the molecular pairs in different directions, while the absence of cylinders along a particular direction is due to weak interactions below a threshold energy (5 kJ/mol) and they are omitted.
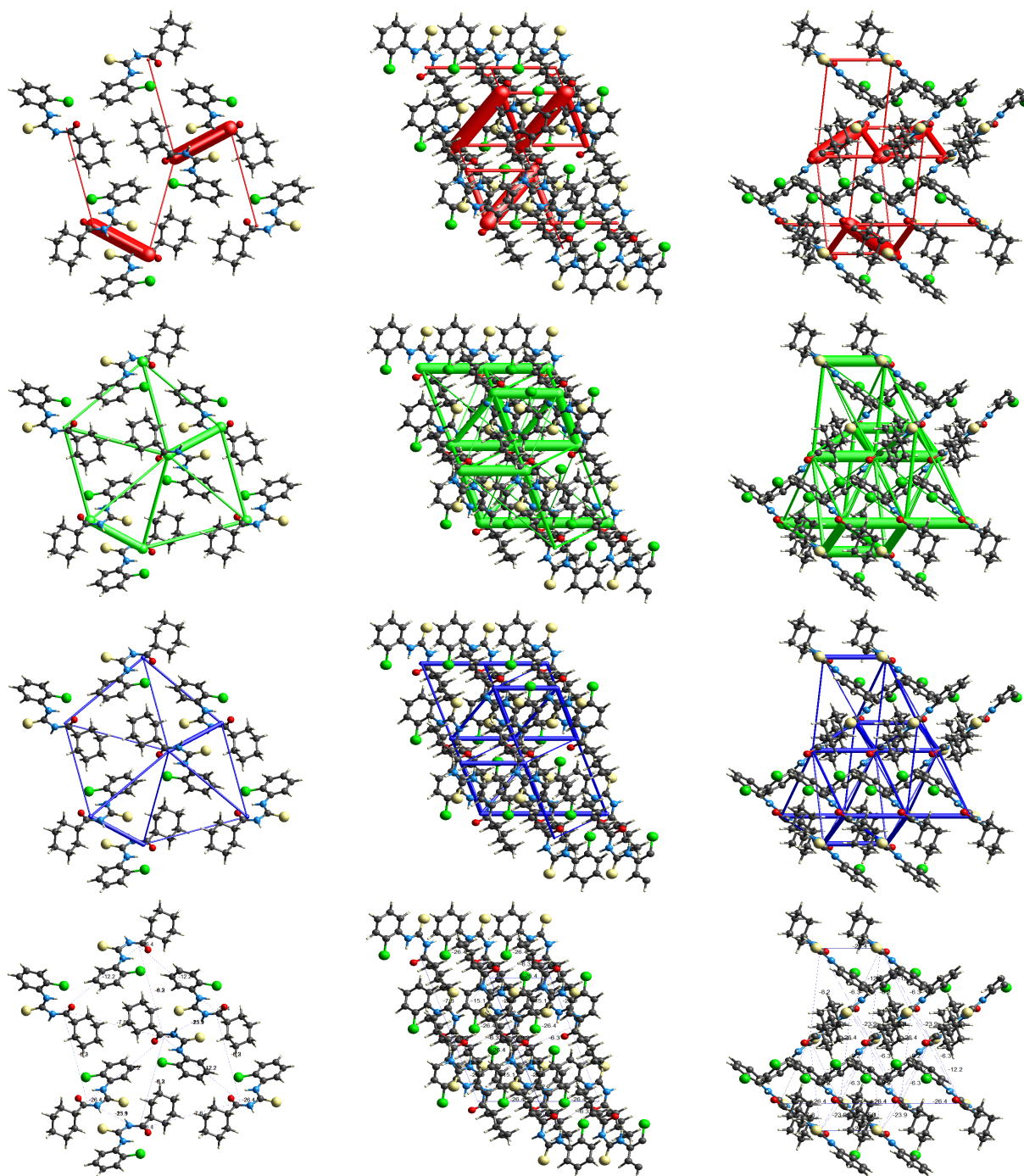
Figure 11. Representation of the Coulomb interaction energy, dispersion energy, and total energy in red, green, and blue colors along the *a, b,* and *c* axes, respectively.

The dispersion energy framework is dominant over the electrostatic energy framework shown in Figure 11 and Table 6. This is due to the presence of a Cl atom, which has a large electron cloud in the title compound [66].

The study of a three-dimensional surface MEP plot is a method to map the electrostatic potential to the isoelectronic density's surface, providing details of the reactive sites. The surface simultaneously shows the molecular size and shape and the electrostatic potential value. The red region indicates an electron-rich region with a partial negative charge and blue region as an electron-deficient region with a partial positive charge in the color scheme. The B3LYP/6-311G(d,p) method was used to obtain the MEP of the title compound. Figure 12

shows that the molecule has two potential electrophilic attack sites. The negative area is located on the carbonyl oxygen atom and the thiocarbonyl sulfur atom. According to Figure 12, the oxygen atom of the C=O group in the title compound is responsible for the nucleophilic attack due to the fact that it has the largest electronegativity among all types of atoms in the title compound. On the other hand, the positive potential sites of the compound are around hydrogen atoms and the most positive point or the blue point is focused around the hydrogen atom of the N-H group which is the most suitable region for susceptible nucleophilic attack [67]. So, the N-H groups in the title compound could act as hydrogen bonding donors.

Table 7. Mulliken atomic charges for the title compound.

Atom	Charge	Atom	Charge	Atom	Charge	Atom	Charge
O1	+0.39319	H10	+0.15875	C19	+0.42756	C28	−0.20717
Cl2	−0.06205	C11	−0.10340	C20	−0.24722	H29	+0.11390
S3	−0.22778	H12	+0.10229	H21	+0.11845	H30	+0.11013
N4	−0.39023	C13	−0.08152	C22	−0.17570	C31	−0.21145
H5	+0.27417	H14	+0.10284	H23	+0.11562	H32	+0.10408
N6	−0.45240	C15	+0.01610	C24	+0.13246	H33	+0.11804
H7	+0.28738	H16	+0.11894	C25	−0.21018	C34	−0.17510
C8	+0.31543	C17	−0.27016	H26	+0.11789	H35	+0.11680
C9	−0.04592	C18	+0.16527	H27	+0.10421	H36	+0.13316
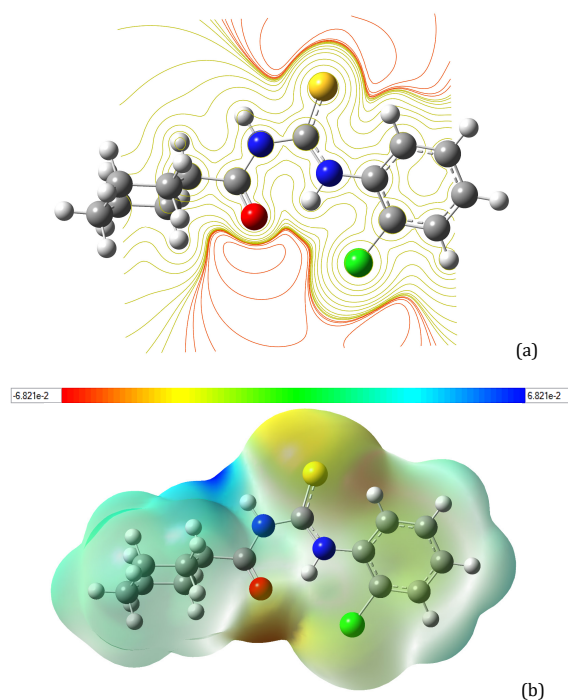
Figure 12. (a) The contour map of electrostatic potential and (b) Molecular electrostatic potential (MEP) map calculated at the B3LYP/6-311G(d,p) level.

The presence of a negative charge on the oxygen, sulphur and chlorine atoms and a positive site on the N–H bonds supports the configuration of H···O, H···S, and H···Cl contacts (Table 4).

In the gas phase at the level of B3LYP/6-311G(d,p), the Mulliken atomic charge of all atoms of the title compound have been obtained by Mulliken atomic charge distribution analysis [68]. While positively charged atoms have the nucleophilic effect, negatively charged atoms are responsible for the electrophilic effect. The values of Mulliken atomic charges are given in Table 7. It is observed that the charge of the N6 atom in the title molecule has the lowest negative value (−0.45240) and the C19 atom has the highest positive value (+0.42756) due to the polarizability of the N-H and C=O groups. These calculated values are in agreement with the intermolecular and intramolecular interactions in the title compound.

5. Conclusions

The title compound was synthesized according to the literature and characterized to confirm its structure. The obtained DFT geometries are in good agreement with the re-refined single crystal X-ray diffraction results. The low energy gap between the frontier molecular orbitals indicates that molecule is unstable with easy transfer of electrons from HOMO to LUMO. In addition, the HOMO-LUMO gap of 3.5399 eV implies that the title compound has good polarizability and high chemical reactivity. The molecular structure is stabilized by different hydrogen bond interactions. Hirshfeld surface studies reveal that the types of intermolecular interactions of the title compound molecule and 2D fingerprint plots present the percentage of each type of contact for it. From the energy 3D frameworks analysis, it is found that the dispersion energy is the dominant factor among all interaction energies, this is due to the presence of the Cl atom which has a large electron cloud in the title compound.

Supporting information Ⓢ

CCDC-2120032 contains the supplementary crystallographic data for this paper. These data can be obtained free of charge via www.ccdc.cam.ac.uk/data_request/cif, or by e-mailing data_request@ccdc.cam.ac.uk, or by contacting The Cambridge Crystallographic Data Centre, 12 Union Road, Cambridge CB2 1EZ, UK; fax: +44(0)1223-336033.

Disclosure statement Ⓓⓢ

Conflict of interest: The authors declare that they have no conflict of interest.
Ethical approval: All ethical guidelines have been adhered.
Sample availability: Sample of the compound is available from the author.

CRediT authorship contribution statement CR

Conceptualization: Hakan Arslan; Methodology: Cemal Koray Ozer, Ummuhan Solmaz, Hakan Arslan; Software: Hakan Arslan; Validation: Ummuhan Solmaz, Hakan Arslan; Formal Analysis: Cemal Koray Ozer, Ummuhan Solmaz, Hakan Arslan; Investigation: Ummuhan Solmaz, Hakan Arslan; Resources: Cemal Koray Ozer; Data Curation: Cemal Koray Ozer, Ummuhan Solmaz, Hakan Arslan; Writing - Original Draft: Ummuhan Solmaz; Writing - Review and Editing: Cemal Koray Ozer, Ummuhan Solmaz, Hakan Arslan; Visualization: Ummuhan Solmaz, Hakan Arslan; Funding acquisition: Hakan Arslan; Supervision: Hakan Arslan; Project Administration: Hakan Arslan.

Funding $

ORCID iD

Cemal Koray Ozer
iD https://orcid.org/0000-0001-9957-4167
Ummuhan Solmaz
iD https://orcid.org/0000-0002-3697-577X
Hakan Arslan
iD https://orcid.org/0000-0003-0046-9442

References

[1]. Karakus, S.; Rollas, S. *Farmaco* **2002**, *57* (7), 577–581.
[2]. Solomon, V. R.; Haq, W.; Smilkstein, M.; Srivastava, K.; Puri, S. K.; Katti, S. B. *Eur. J. Med. Chem.* **2010**, *45* (11), 4990–4996.
[3]. Saeed, A.; Flörke, U.; Erben, M. F. *J. Sulphur Chem.* **2014**, *35* (3), 318–355.
[4]. Beyer, L.; Hoyer, E.; Liebscher, J.; Hartmann, H. *Z. Chem.* **2010**, *21* (3), 81–91.
[5]. Mühl, P.; Gloe, K.; Dietze, F.; Hoyer, E.; Beyer, L. *Z. Chem.* **2010**, *26* (3), 81–94.
[6]. Duque, J.; Estevez-Hernandez, O.; Reguera, E.; Ellena, J.; Correa, R. S. *J. Coord. Chem.* **2009**, *62* (17), 2804–2813.
[7]. Estevez-Hernandez, O.; Duque, J.; Rodríguez-Hernandez, J.; Reguera, E. *Polyhedron* **2015**, *97*, 148–156.
[8]. Yesilkaynak, T. *J. Therm. Anal. Calorim.* **2016**, *124* (2), 1029–1037.
[9]. Correa, R. S.; de Oliveira, K. M.; Delolo, F. G.; Alvarez, A.; Mocelo, R.; Plutin, A. M.; Cominetti, M. R.; Castellano, E. E.; Batista, A. A. *J. Inorg. Biochem.* **2015**, *150*, 63–71.
[10]. Sternberg, M.; Rust, J.; Lehmann, C. W.; Mohr, F. *Helv. Chim. Acta* **2013**, *96* (2), 280–288.
[11]. Hassan, S. S.; Shoukry, M. M.; Shallan, R. N.; van Eldik, R. *J. Coord. Chem.* **2017**, *70* (10), 1761–1775.
[12]. Hussain, S.; Imtiaz-ud-Din; Raheel, A.; Hussain, S.; Tahir, M. N.; Hussain, I. *J. Coord. Chem.* **2020**, *73* (7), 1191–1207.
[13]. Teixeira, E. I.; Schwalm, C. S.; Casagrande, G. A.; Tirloni, B.; Schwade, V. D. *J. Mol. Struct.* **2020**, *1210* (127999), 127999.
[14]. Barnard, I.; Koch, K. R.; Gerber, W. J. *J. Mol. Struct.* **2021**, *1244* (131009), 131009.
[15]. Lapasam, A.; Kollipara, M. R. *Phosphorus Sulfur Silicon Relat. Elem.* **2020**, *195* (10), 779–804.
[16]. Ketchemen, K. I. Y.; Khan, M. D.; Mlowe, S.; Akerman, M. P.; Vitorica-Yrezabal, I.; Whitehead, G.; Nyamen, L. D.; Ndifon, P. T.; Revaprasadu, N.; O'Brien, P. *J. Mol. Struct.* **2021**, *1229* (129791), 129791.
[17]. Cunha, B. N.; Luna-Dulcey, L.; Plutin, A. M.; Silveira, R. G.; Honorato, J.; Cairo, R. R.; de Oliveira, T. D.; Cominetti, M. R.; Castellano, E. E.; Batista, A. A. *Inorg. Chem.* **2020**, *59* (7), 5072–5085.
[18]. Nkabyo, H. A.; Barnard, I.; Koch, K. R.; Luckay, R. C. *Coord. Chem. Rev.* **2021**, *427* (213588), 213588.
[19]. Tudor, C. A.; Iliş, M.; Secu, M.; Ferbinteanu, M.; Cîrcu, V. *Polyhedron* **2022**, *211* (115542), 115542.
[20]. Mitrea, D. G.; Circu, V. *Spectrochim. Acta A Mol. Biomol. Spectrosc.* **2021**, *258* (119860), 119860.
[21]. Plutín, A. M.; Ramos, R.; Mocelo, R.; Alvarez, A.; Castellano, E. E.; Cominetti, M. R.; Oliveira, K. M.; Donizeth de Oliveira, T.; Silva, T. E. M.; S. Correa, R.; Batista, A. A. *Polyhedron* **2020**, *184* (114543), 114543.
[22]. Yuan, Y. F.; Wang, J. T.; Gimeno, M. C.; Laguna, A.; Jones, P. G. *Inorganica Chim. Acta* **2001**, *324* (1–2), 309–317.
[23]. Zhang, Y. M.; Wei, T. B.; Xian, L.; Gao, L. M. *Phosphorus Sulfur Silicon Relat. Elem.* **2004**, *179* (10), 2007–2013.
[24]. You-Ming, Z.; Tai-Bao, W.; Xiu-Chun, W.; Su-You, Y. *Indian J. Chem.* **1998**, *37B*, 604–606.
[25]. Weiqun, Z.; Baolong, L.; Liming, Z.; Jiangang, D.; Yong, Z.; Lude, L.; Xujie, Y. *J. Mol. Struct.* **2004**, *690* (1–3), 145–150.
[26]. Ozer, C. K.; Binzet, G.; Arslan, H. *Eur. J. Chem.* **2020**, *11* (4), 319–323.
[27]. Ozer, C. K.; Arslan, H.; VanDerveer, D.; Külcü, N. *Molecules* **2009**, *14* (2), 655–666.
[28]. Arslan, B., MSc Thesis, Mersin University, Mersin, Turkey, 2017.
[29]. Binzet, G.; Arslan, H.; Flörke, U.; Külcü, N.; Duran, N. *J. Coord. Chem.* **2006**, *59* (12), 1395–1406.
[30]. Arslan, H.; Flörke, U.; Külcü, N.; Emen, M. F. *J. Coord. Chem.* **2006**, *59* (2), 223–228.
[31]. Binzet, G.; Gumus, I.; Dogen, A.; Flörke, U.; Kulcu, N.; Arslan, H. *J. Mol. Struct.* **2018**, *1161*, 519–529.
[32]. Arslan, H.; Flörke, U.; Külcü, N. *Acta Crystallogr. Sect. E Struct. Rep. Online* **2003**, *59* (5), o641–o642.
[33]. Arslan, H.; Flörke, U.; Külcü, N. *J. Chem. Crystallogr.* **2003**, *33* (12), 919–924.
[34]. Ozpozan, N.; Arslan, H.; Ozpozan, T.; Merdivan, M.; Külcü, N. *J. Therm. Anal. Calorim.* **2000**, *61* (3), 955–965.
[35]. Solmaz, U.; Gumus, I.; Yilmaz, M. K.; Ince, S.; Arslan, H. *Appl. Organomet. Chem.* **2021**, *35* (10), e6348.
[36]. Dolomanov, O. V.; Bourhis, L. J.; Gildea, R. J.; Howard, J. A. K.; Puschmann, H. *J. Appl. Crystallogr.* **2009**, *42* (2), 339–341.
[37]. Palatinus, L.; Chapuis, G. *J. Appl. Crystallogr.* **2007**, *40* (4), 786–790.
[38]. Palatinus, L.; van der Lee, A. *J. Appl. Crystallogr.* **2008**, *41* (6), 975–984.
[39]. Palatinus, L.; Prathapa, S. J.; van Smaalen, S. *J. Appl. Crystallogr.* **2012**, *45* (3), 575–580.
[40]. Sheldrick, G. M. *Acta Crystallogr. C Struct. Chem.* **2015**, *71* (Pt 1), 3–8.
[41]. Frisch, M. J.; Trucks, G. W.; Schlegel, H. B.; Scuseria, G. E.; Robb, M. A.; Cheeseman, J. R.; Scalmani, G.; Barone, V.; Petersson, G. A.; Nakatsuji, H.; Li, X.; Caricato, M.; Marenich, A. V.; Bloino, J.; Janesko, B. G.; Gomperts, R.; Mennucci, B.; Hratchian, H. P.; Ortiz, J. V.; Izmaylov, A. F.; Sonnenberg, J. L.; Williams-Young, D.; Ding, F.; Lipparini, F.; Egidi, F.; Goings, J.; Peng, B.; Petrone, A.; Henderson, T.; Ranasinghe, D.; Zakrzewski, V. G.; Gao, J.; Rega, N.; Zheng, G.; Liang, W.; Hada, M.; Ehara, M.; Toyota, K.; Fukuda, R.; Hasegawa, J.; Ishida, M.; Nakajima, T.; Honda, Y.; Kitao, O.; Nakai, H.; Vreven, T.; Throssell, K.; Montgomery, J. A., Jr.; Peralta, J. E.; Ogliaro, F.; Bearpark, M. J.; Heyd, J. J.; Brothers, E. N.; Kudin, K. N.; Staroverov, V. N.; Keith, T. A.; Kobayashi, R.; Normand, J.; Raghavachari, K.; Rendell, A. P.; Burant, J. C.; Iyengar, S. S.; Tomasi, J.; Cossi, M.; Millam, J. M.; Klene, M.; Adamo, C.; Cammi, R.; Ochterski, J. W.; Martin, R. L.; Morokuma, K.; Farkas, O.; Foresman, J. B.; Fox, D. J. Gaussian 16, Revision C.01, Gaussian, Inc., Wallingford CT, 2016.
[42]. Becke, A. D. *J. Chem. Phys.* **1993**, *98* (7), 5648–5652.
[43]. Lee, C. T.; Yang, W.T.; Parr, R.G. *Phys. Rev. B.* **1988**, *37* (2), 785–789.
[44]. Dennington, R.; Keith, T. A.; Millam, J. M. GaussView, Version 6, Semichem Inc., Shawnee Mission, KS, 2016.
[45]. McKinnon, J. J.; Jayatilaka, D.; Spackman, M. A. *Chem. Commun. (Camb.)* **2007**, No. 37, 3814–3816.
[46]. Spackman, M. A.; Jayatilaka, D. *CrystEngComm* **2009**, *11* (1), 19–32.
[47]. Spackman, P. R.; Turner, M. J.; McKinnon, J. J.; Wolff, S. K.; Grimwood, D. J.; Jayatilaka, D.; Spackman, M. A. *J. Appl. Cryst.* **2021**, *54* (3), 1006–1011.
[48]. Spackman, M. A.; McKinnon, J. J. *CrystEngComm* **2002**, *4* (66), 378–392.
[49]. Spackman, M. A.; McKinnon, J. J.; Jayatilaka, D. *CrystEngComm* **2008**, *10* (4), 377–388.
[50]. Jayatilaka, D.; Grimwood, D. J. Tonto: A FORTRAN Based Object-Oriented System for Quantum Chemistry and Crystallography. In *Lecture Notes in Computer Science*; Springer Berlin Heidelberg: Berlin, Heidelberg, 2003; pp 142–151.
[51]. Allen, F. H.; Kennard, O.; Watson, D. G.; Brammer, L.; Guy Orpen, A.; Taylor, R. *J. Chem. Soc. Perkin Trans. 2* **1987**, *12*, S1–S19.
[52]. Arslan, H.; Külcü, N.; Flörke, U. *Spectrochim. Acta A Mol. Biomol. Spectrosc.* **2006**, *64* (4), 1065–1071.
[53]. Arslan, H.; Florke, U.; Kulcu, N.; Kayhan, E. *Turk. J. Chem* **2006**, *30*, 429–440.
[54]. Khawar Rauf, M.; Badshah, A.; Bolte, M. *Acta Crystallogr. Sect. E Struct. Rep. Online* **2007**, *63* (4), o1676–o1678.

[55]. Arslan, H.; Florke, U.; Kulcu, N. *Acta Chim. Slov* **2004**, *51*, 787–792.

[56]. Shen, X.; Shi, X.; Kang, B.; Tong, Y.; Liu, Y.; Gu, L.; Liu, Q.; Huang, Y. *Polyhedron* **1998**, *18* (1–2), 33–37.

[57]. Yamin, B. M.; Yusof, M. S. M. *Acta Crystallogr. Sect. E Struct. Rep. Online* **2003**, *59* (2), o151–o152.

[58]. Yusof, M. S. M.; Asroh, F. S. M.; Kadir, M. A.; Yamin, B. M. *Acta Crystallogr. Sect. E Struct. Rep. Online* **2007**, *63* (3), o1190–o1191.

[59]. Cremer, D.; Pople, J. A. *J. Am. Chem. Soc.* **1975**, *97* (6), 1354–1358.

[60]. Evans, D. G.; Boeyens, J. C. A. *Acta Crystallogr. B* **1989**, *45* (6), 581–590.

[61]. Chermette, H. *J. Comput. Chem.* **1999**, *20* (1), 129–154.

[62]. Baumgärtner, A. *J. Chem. Phys.* **1993**, *98* (9), 7496–7501.

[63]. Bogolubov, N. N. Jr; Kien, F. L.; Shumovsky, A. S. *J. Phys. A Math. Gen.* **1986**, *19* (2), 191–203.

[64]. Meyer, A. Y. *Chem. Soc. Rev.* **1986**, *15* (4), 449-474.

[65]. Mackenzie, C. F.; Spackman, P. R.; Jayatilaka, D.; Spackman, M. A. *IUCrJ* **2017**, *4* (Pt 5), 575–587.

[66]. Edwards, A. J.; Mackenzie, C. F.; Spackman, P. R.; Jayatilaka, D.; Spackman, M. A. *Faraday Discuss.* **2017**, *203*, 93–112.

[67]. Scrocco, E.; Tomasi, J. The Electrostatic Molecular Potential as a Tool for the Interpretation of Molecular Properties. In *Topics in Current Chemistry Fortschritte der Chemischen Forschung*; Springer Berlin Heidelberg: Berlin, Heidelberg, 2007; pp 95–170.

[68]. Mulliken, R. S. *J. Chem. Phys.* **1955**, *23* (10), 1833–1840.